A Concurrent Multi-band Power Amplifier with Compact Matching Networks

Atsushi Fukuda[1], *Hiroshi Okazaki*[1], *Shoichi Narahashi*[1], *and Toshio Nojima*[2]

[1]Research Laboratories, NTT DOCOMO, INC., 3-5 Hikarino-oka, Yokosuka, Kanagawa, 239-8536, Japan
Email: fukudaat@nttdocomo.co.jp

[2]Graduate School of Information Science and Technology, Hokkaido University, Kita 14, Nishi 9, Kita-ku, Sapporo, Hokkaido, 060-0814, Japan

Abstract

This paper presents a novel configuration for a concurrent multi-band power amplifier (PA). A multi-band matching network comprises a multi-section impedance transformer that achieves matching in multiple bands. The proposed impedance transformer provides flexibility in the design of a concurrent multi-band PA in a wide frequency range. The impedance transformer is compact since each section comprises a combination of a T-shaped network, a shunt tank circuit, and a matching element. The proposed 1W-class dual-band PA achieves a maximum power added efficiency of greater than 53% at 0.8 GHz and 3.3 GHz.

1. Introduction

Recently, radio frequency (RF) components for mobile communications have been developed to operate seamlessly using different wireless communication standards and frequency bands that are in use all over the world. In addition, a wide operating band is required for next generation systems due to the demand for high-speed and high-capacity transmission. One candidate to obtain a wide operating band is spectrum aggregation technology [1], which employs several bands aggregately and concurrently. One technical issue is configuring RF components with concurrent operation in multiple bands without significantly increasing the circuit size.

A power amplifier (PA) is a primary device in RF components. It is difficult for PAs to operate concurrently in multiple bands with adequate performance in terms of, for example, high output power and high efficiency due to the inherent narrow band characteristics of matching networks (MNs). There are two kinds of configurations for PAs with concurrent operation in multiple bands [2-6]. One approach employs "broadband MNs" that are designed to work in a wide range of frequencies [2-3]. However, broadband MNs have difficulties in achieving the appropriate matching for highly efficient operation in each band when the upper and lower limits of the required bands are far apart. The other configuration employs "multi-band MNs" (MB-MNs) that achieve matching concurrently in multiple individual bands [4-6]. A Chebyshev-form impedance transformer [7] was adopted into a dual-band PA [4]. A multi-section impedance transformer with tank circuits [5] or branched stubs [6] achieved matching concurrently in multiple bands. In [5], series and parallel reactive circuits in a section of the transformer are designed not only to match in an individual band but also to avoid impedance deviation in the matched bands before the section. To satisfy the latter condition, a transmission line with a characteristic impedance that equals the source/load impedance is required for the series circuit [5]. The length of the transmission line may occupy a large area in the MN.

This paper proposes a novel MB-MN configuration employing the multi-section impedance transformer reported in [5]. The proposed configuration employs a lumped T-shaped network instead of the transmission line for the MB-MN. A 1W class 0.8/3.3 GHz dual-band PA is fabricated to investigate the effectiveness of the proposed configuration. Measurement results show that the dual-band PA achieves a maximum power added efficiency (PAE) of over 53% and an output power exceeding 30 dBm at individual frequencies.

2. Proposed Configuration for Multi-band Matching Network

The configuration of the previously reported MB-MN in [5] is shown in Fig. 1. N is the number of operating bands. Here, the n-th band, B_n ($1 \le n \le N$), with the center frequency of f_n is allocated in accordance with $B_1 > \cdots > B_N$. The highest band, B_1, is allocated to the first MN since the proposed configuration adapts the low-pass type MN. A

978-1-4244-6051-9/11/$26.00 ©2011 IEEE

multi-section impedance transformer with N-1 sections matches in the other bands. The (m-1)-th (2≤m≤N) section in the transformer is also a low-pass type MN that comprises a transmission line with the length of $d_{(m-1)}$ and a shunt block with the reactance of $X_{(m-1)}(f_n)$. In Fig. 1, $d_{(m-1)}$ and $X_{(m-1)}(f_m)$ are designed to transform the impedance at f_m at point m-1, $Z_{m-1}(f_m)$, to the load impedance, Z_0. Here, each band between B_1 and B_{m-1} has been matched to Z_0 before designing the (m-1)-th section. To avoid impedance deviation in the matched bands, the characteristic impedance of the transmission line and $X_{(m-1)}(f_1)$, · · · , $X_{(m-1)}(f_{m-1})$ are set to Z_0 and infinity, respectively.

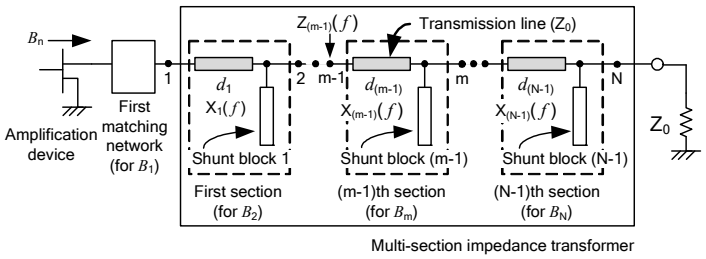

Fig. 1 Basic topology of multi-section multi-band matching network (for output).

When operating bands are allocated in a wide frequency range, the physical length of the transmission line may become long, in particular, in low bands below 1 GHz. A newly proposed configuration for the transformer shown in Fig. 2 employs a T-shaped network instead of the long transmission line to decrease the circuit size. The T-shaped network avoids the impedance deviation in the matched bands at point m-1 in Fig. 2. A practical configuration example for dual-band operation is shown in Fig. 3. In the first section, the T-shaped network works not only as the network matched to Z_0 at f_1 but the specified inductor for matching $Z_1(f_2)$ in Fig. 2 to Z_0 at f_2 when the shunt capacitance is small. On the other hand, the shunt block in Fig. 2 is configured by a cascade connection of a tank circuit and a matching capacitor for B_2. Here, the resonant frequency of the tank circuit, f_r, equals f_1. Then, $X_1(f)$ in Fig. 2 is set to be infinite at f_1 and is set to the desired reactance for matching at f_2. The $Z_1(f_1)$ matched to Z_0 by the first MN is kept constant until point 2 in Fig. 3 and $Z_1(f_2)$ is transformed to Z_0 at point 2 in Fig. 3, namely $Z_2(f_1)=Z_2(f_2)=Z_0$ is achieved simultaneously.

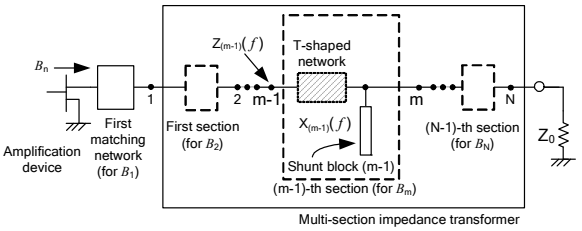

Fig. 2 Newly proposed configuration (for output).

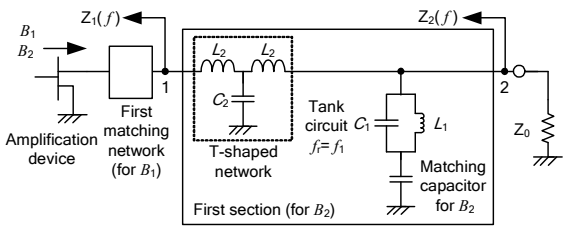

Fig. 3 Practical configuration (for output).

3. Design and Testing of Proposed PA

To confirm the feasibility of the proposed MB-MN configuration, a dual-band PA is designed for the 0.8-GHz, and 3.3-GHz bands. The first MN is designed for the 3.3-GHz band because of the higher band. The following section is designed for the 0.8-GHz band. The tank circuit with inductance L_1 and capacitance C_1 is designed to have a resonant frequency of f_r = 3.3 GHz. Then, as X_1 (f= 3.3 GHz) becomes infinite, the tank circuit acts as an off-state switch in the 3.3-GHz band. According to the identified $Z_1(f$= 0.8 GHz) from the first MN configuration, the T-shaped network with inductance L_2 is set for matching in the 0.8-GHz band and capacitance C_2 is set to avoid impedance deviation in the 3.3-GHz band.

From experimental investigations, the input MN uses chip inductors and chip capacitors with the values of L_1=1.2 nH, L_2=3.6 nH, C_1=1.3 pF, and C_2=0.5 pF, and the output MN uses L_1=1.2 nH, L_2=4.3 nH, C_1=1.3 pF, and C_2=0.4 pF. Figure 4 depicts the S parameter measurement configuration for the tank circuit and the T-shaped network implemented in a 50 Ω system. Figures 5, 6(a), and 6(b) show measured frequency responses of the shunt tank circuit and T-shaped networks for input and output MNs, respectively. The figures include a 0.3-dB loss for the feed transmission line and connectors. As shown in Fig. 5, the tank circuit achieves S11 and S21 characteristics of

−28 dB and −0.5 dB at 3.3 GHz, respectively. The figure also shows that the bandwidth of 615 MHz centered at 3.24 GHz has S11 characteristics of below −15 dB. According to Figs. 6(a) and 6(b), at 3.3 GHz the T-shaped network achieves S11 and S21 characteristics of −21 dB and −0.6 dB for the input MN and −26 dB and −0.7 dB for the output MN, respectively. These figures also indicate that the S11 characteristics in the 3.3-GHz band are below −15 dB for the bandwidths of 348 MHz for the input MN and 215 MHz for the output MN.

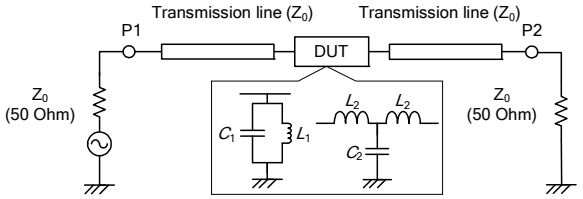

Fig. 4 Measurement configuration.

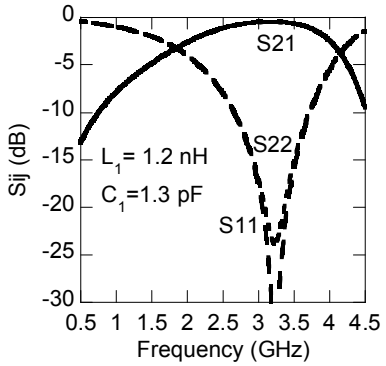

Fig. 5 Measured frequency response of tank circuit.

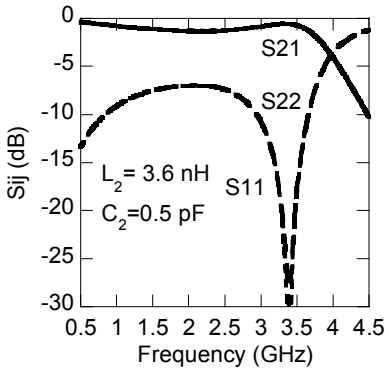

(a)

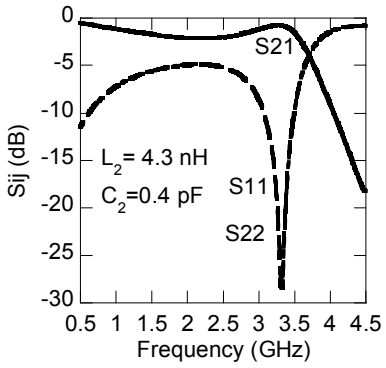

(b)

Fig. 6 Measured frequency response of T-shaped network for (a) input and (b) output MNs.

The 0.8-GHz/ 3.3-GHz single stage dual-band PA is fabricated. The size of the printed circuit board is 50 mm x 60 mm. The dielectric constant and total thickness of the substrate is 2.2 and 0.785 mm, respectively. A commercially available GaAs MESFET is employed. The lumped components for MB-MNs are deployed on both sides of the transistor. A photograph of the fabricated dual-band PA is shown in Fig. 7.

Figure 8 shows the measured frequency response of the fabricated dual-band PA based on small signal S-parameters. As shown in Fig. 8, the dual-band PA achieves a gain exceeding 13 dB and 9 dB in the 0.8-GHz and 3.3-GHz operating bands, respectively. The FET is biased to a class-AB operation of V_{GS}= −2V and V_{DS}= 10V. From Fig. 8, the matching conditions of the input and output terminals are good for each of the two desired bands.

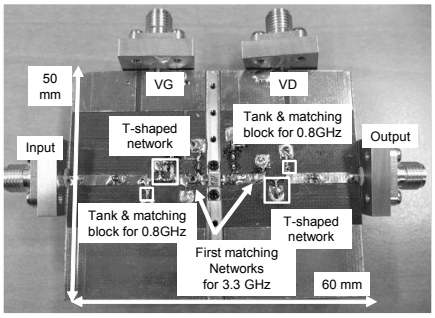

Fig. 7 Photograph of fabricated dual-band PA.

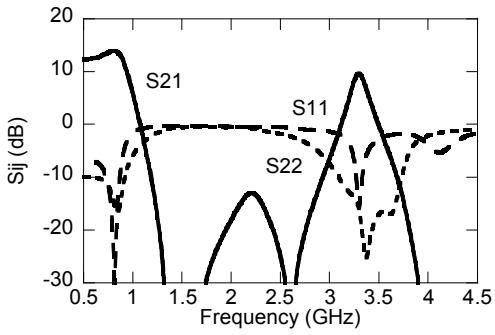

Fig. 8 Measured frequency response of dual-band PA.

Figure 9 shows the output power and PAE at various single tone input powers at (a) 0.8 GHz and (b) 3.3 GHz. The maximum PAE levels at the two frequencies are 62% and 53% with the associated gain of 12 dB and 8 dB, respectively. The saturated output powers at the two frequencies are 30.1 dBm and 30.5 dBm, respectively. The output powers at 1-dB gain compression point at the two frequencies are 28.7 dBm and 29.4 dBm, respectively.

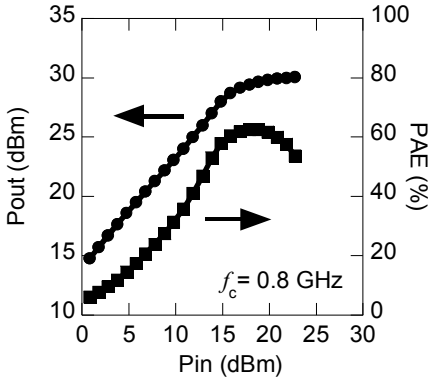

(a) 0.8 GHz

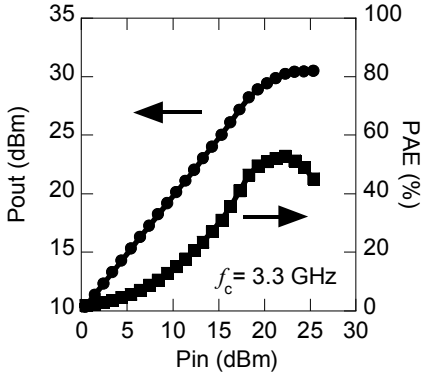

(b) 3.3 GHz

Fig. 9 Measured output power and PAE characteristics measured at (a) 0.8 GHz and (b) 3.3 GHz.

4. Conclusion

This paper presented a compact configuration for the MB-MN that employs a multi-section impedance transformer. The transformer with a T-shaped network and tank circuits achieves matching in multiple bands concurrently. Employing chip inductors instead of the transmission line makes the concurrent multi-band PA compact. Experimental results confirm that the proposed MN can be successfully operated with high efficiency in dual bands in a wide frequency range, e.g., 0.8 GHz and 3.3 GHz. A future research topic is to examine the feasibility of increasing the number of operating bands to more than two bands and employing a multi-stage PA with an adequate gain.

5. References

1. D. L. Robinson, A. K. Shukla, J. Burns, and A. Atefi, "Resource Trading for Spectrum Aggregation and Management," in Proc. DySPAN 2005, Nov. 2005, pp. 666-671.

2. I. J. Bahl, "0.7-2.7-GHz 12-W Power-Amplifier MMIC Developed Using MLP Technology," IEEE Trans. Microwave Theory and Tech., vol. 55, Feb. 2007, pp. 222–229.

3. S. Azam, R. Jonsson, and Q. Wahab, "Designing, Fabrication and Characterization of Power Amplifiers Based on 10-Watt SiC MESFET & GaN HEMT at Microwave Frequencies," in Proc. 38th EuMC, Sep. 2008, pp. 444–447.

4. K. Uchida, Y. Takayama, T. Fujita, and K. Maenaka, "Dual-band GaAs FET Power Amplifier with Two-Frequency Matching Circuits," in 2002 Asia-Pacific Microwave Conference Workshop, WS8-2, Dec. 2005.

5. A. Fukuda, H. Okazaki and S. Narahashi, "Novel Multi-Band Matching Scheme for Highly Efficient Power Amplifier," in Proc. 39th EuMC, Sept. 2009, pp. 1086–1089.

6. A. Fukuda, H. Okazaki, S. Narahashi and T. Nojima, "Concurrent Multi-band Power Amplifier Employing Multi-section Impedance Transformer," in Proc. 2011 IEEE Radio and Wireless Symposium (RWS), Jan. 2011, pp. 37–40.

7. G. L. Matteai, "Tables of Chebyshev Impedance-Transforming Networks of Low-Pass Filter Form," proc. IEEE, Aug. 1964, pp. 939-963.